

Received December 3, 2019, accepted December 12, 2019, date of publication December 18, 2019, date of current version December 31, 2019.

Digital Object Identifier 10.1109/ACCESS.2019.2960639

Wide-Angle Beam Steering Based on an Active Conformal Metasurface Lens

HUAN LI¹, CHAO MA¹, FAZHONG SHEN¹, KUIWEN XU^{1,4}, DEXIN YE¹,
JIANGTAO HUANGFU¹, CHANGZHI LI², (Senior Member, IEEE), LIXIN RAN¹,
AND TAYEB A. DENIDNI³, (Fellow, IEEE)

¹Laboratory of Applied Research on Electromagnetics (ARE), Zhejiang University, Hangzhou 310027, China

²Department of Electrical and Computer Engineering, Texas Tech University, Lubbock, TX 79424, USA

³Institut National de la Recherche Scientifique, University of Quebec, Montreal, QC H5A1K6, Canada

⁴Key Laboratory of RF Circuits and Systems of the Ministry of Education of China, Hangzhou Dianzi University, Hangzhou 310018, China

Corresponding author: Tayeb A. Denidni (denidni@emt.inrs.ca)

This work was supported in part by the NSFC under Grant 61701437, Grant 61771421, Grant 51607168, Grant 61771422, and Grant 61601161, in part by the Aeronautical Science Foundation of China under Grant ASFC-2017ZC76002, and in part by the China Postdoctoral Science Foundation under Grant 2017M611989.

ABSTRACT This work experimentally demonstrates a wide-angle beam steering based on an active conformal metasurface lens. Integrated with microwave varactors, the transmission phase of this cylindrical metasurface lens can be tuned in a range up to 195° by direct-current (DC) bias voltages. By compensating the phase difference between different incidences, the proposed cylindrical lens can collimate the incident spherical wave front into a plane wave front with predefined deflection angle. By increasing the number of feeding sources, the beam steering range of conformal lens can be expanded to $\pm 60^\circ$. Having advantages of low cost and simple structure, the proposed conformal lens can be extended to millimeter-wave band and enable a wide range of applications.

INDEX TERMS Conformal antenna, active metasurface, phase shift, beam steering, cylindrical lens.

I. INTRODUCTION

Having the ability of flexible control of beam direction, phased array antennas have been used in a wide range of applications such as satellite communications and radars. However, they suffer from high costs due to the requirement of complex feeding and phase shifting networks [1]–[3]. Recently, several new techniques have been proposed to implement beam steering antennas. Examples include antenna systems based on tunable impedance surfaces [4]–[6], ferroelectric ceramic [7], photo-sensitive semiconductors [8], [9], tunable metamaterials [10]–[16], coding metasurfaces [17]–[19], and frequency selective surfaces (FSSs) [20]–[22], and reconfigurable Fresnel zone plate (FZP) at single and dual bands [23], [24]. Among these new-concept antennas, FZP antennas [23], [24] can achieve a scanning range of $\pm 30^\circ$ with simple structures. However, due to the lack of phase compensation ability, the side lobe level (SLL) of existing FZP antennas is not satisfactory. The phase-correction technique, either partial phase or full phase, has been demonstrated as an effective method to suppress the

side lobe of FZP antennas [25], [26]. Employing metamaterials or FSSs as spatial phase shifters, several lens antennas with passive phase corrections have been proposed to collimate the incident spherical waves into plane waves [27]–[30]. By rotating the lens [31] or adjusting the position of feeding source [32], mechanically steerable lens antennas have also been demonstrated. In [33], to obtain multiple discrete beams, seven feeding elements were used to illuminate a planar metamaterial lens, achieving a beam coverage of $\pm 27^\circ$.

On the other hand, to increase the beam steering range of phased array antennas, one method is to place the radiating elements on conformal surfaces, such as cylindrical [34] and spherical surfaces [35]. Implementing beam steering antennas on conformal surfaces are also desirable in order to meet the aerodynamic requirements in some communication platforms, such as aircrafts and satellites [35]. However, in addition to the complexity and high costs, the design and fabrication of a phased array antenna on a conformal aperture are more challenging compared with a planar one.

In this work, a wide-angle beam steering antenna is experimentally demonstrated based on an active conformal metasurface lens. Integrated with microwave varactors, the transmission phase of this cylindrical conformal lens can

The associate editor coordinating the review of this manuscript and approving it for publication was Kwok L. Chung¹.

TABLE 1. Phase distribution at different columns for 0° deflection angle.

Column No.	1	2	3~4	5	6	7~8	9	10	11~13	14	15	16	17	18~25
$\Delta\varphi$	284°	196°	< 195°	295°	211°	< 195°	331°	256°	< 195°	351°	295°	243°	196°	< 195°
Φ	89°	1°	0°	100°	16°	0°	136°	61°	0°	156°	100°	48°	1°	0°

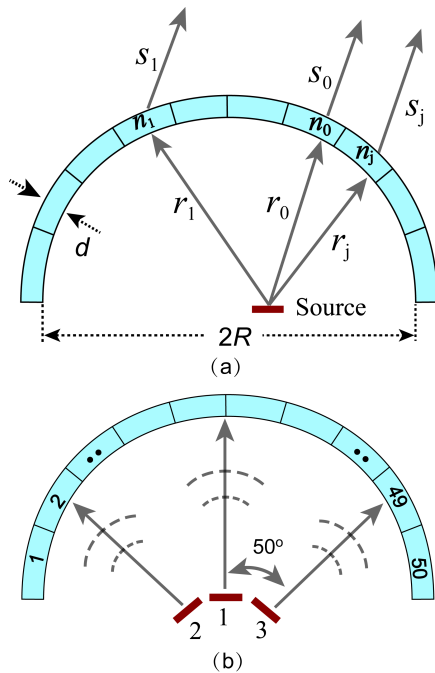


FIGURE 1. Beam steering principle of conformal cylindrical lens antenna. (a) Single feeding antenna. (b) Multiple feeding antennas.

be tuned in a range up to 195° by direct-current (DC) bias voltages. By compensating the phase difference between different incidences, it can collimate the incident spherical wave front into a plane wave front with predefined deflection angle. Utilizing three patch antennas as multiple feeding sources, the proposed conformal lens antennas can achieve a scanning coverage of ± 60°. Compared with previous reconfigurable planar FZP antennas [23], [24], the proposed conformal lens antenna has lower side lobe and larger scanning range.

This paper is organized as follows. In section II, the beam steering principle of cylindrical lens antenna is introduced. In section III, the design and simulation of active metasurface lens are described. Experimental results of wide-angle beam steering are given in section IV. Finally, a conclusion is drawn in section V.

II. PRINCIPLE

The beam steering principle of conformal cylindrical lens antenna is shown in Fig. 1(a), in which a cylindrical wave illumination is considered. Due to the rotation symmetric feature, multiple feeding sources can be used to illuminate the cylindrical lens, as shown in Fig.1(b). With an inner radius

R and a thickness of d , the conformal lens is divided into N subwavelength segments. Assuming the transmission phase of each segment can be individually controlled (in this work by DC voltages applied to the varactors in metasurface unit cells), the transformation of a cylindrical wave front into a planar wave front with a predefined deflection angle can be understood based on the geometric-optics method. The shortest ray that arrives in the desired S_0 direction, i.e. $r_0 + S_0$, is assigned as the reference ray. Then the phase difference $\Delta\varphi$ between vector rays S_1 and S_0 can be written as

$$\Delta\varphi = k_0[(|r_1 + |S_1|) - (|r_0 + |S_0|)] \quad (1)$$

where k_0 is the free-space wave vector. By compensating the phase differences between different rays passing through divided segments, the outgoing wave can be collimated to the predefined direction.

In order to verify the above mechanism, two-dimensional simulations are performed with Comsol Multiphysics simulator. As an example, we consider a half cylindrical lens with $R = 200$ mm, $d = 6$ mm, and $N = 50$. The cylindrical wave excitation with transverse magnetic (TM) polarization is generated by an open-end waveguide antenna, as shown in Fig. 2(a). In the simulation, each segment is assumed as homogeneous substrate and the phase shift caused by this segment is controlled by tuning its refractive index. The phase difference $\Delta\varphi$ is related to the refractive index difference Δn by $\Delta\varphi = k_0 d \Delta n$, where $\Delta n = n_1 - n_0$. The simulation is performed at 5.75 GHz and the phase tunability is assumed as 195°, which complies with the experimentally measured tunability in this work, as will be demonstrated in the following. In the simulation, for rays with phase differences larger than 195° but less than 360°, a maximum 195° phase shift is used to achieve partial phase compensation. For rays with phase differences $\Delta\varphi$ less than 195°, a $-\Delta\varphi$ phase shift is used to achieve full phase compensation. As an example, table 1 shows a sequence of phases at different columns when the beam deflection angle is 0°. In table 1, $\Delta\varphi$ denotes the calculated phase difference according to formula (1) while Φ represents the phase values at different columns after phase compensation. Due to the symmetric structure of cylindrical lens, the phase distribution at 1~25 columns are given in table 1.

Figures 2(a) and 2(b) show the near field distributions for beams deflected to 0° and 25°, respectively. In these cases, the feeding antenna is located at the center of cylindrical lens, so that the incident wave front coincides with the conformal lens. Since 195° phase tunability can partially satisfy the

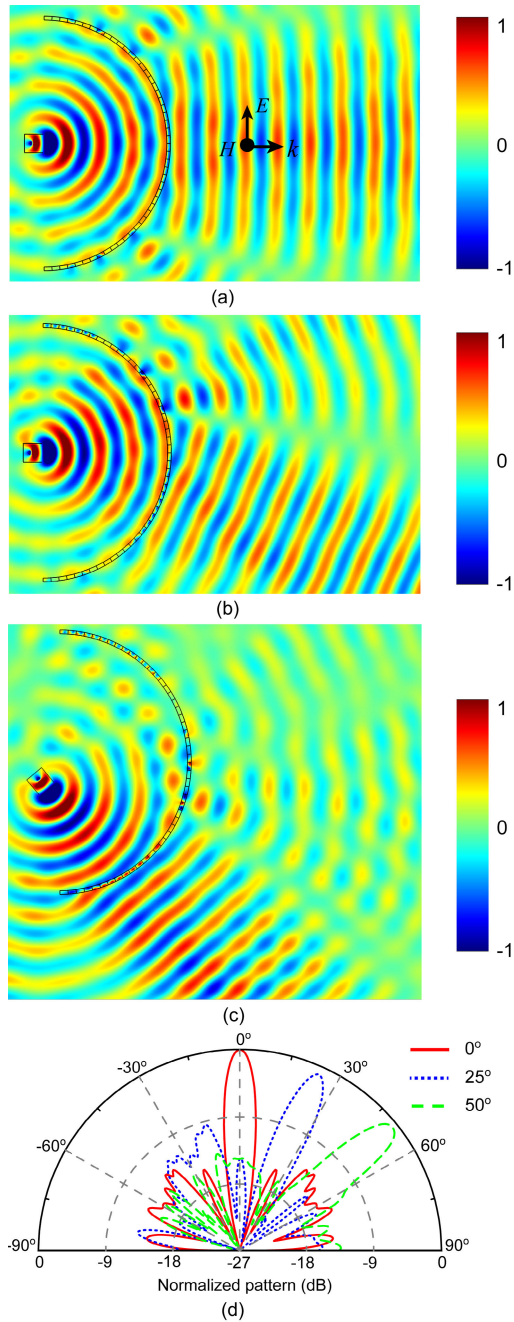


FIGURE 2. Simulated results of the cylindrical lens antenna by Comsol. Near field distribution for lens antenna with beam deflection at (a) 0°, (b) 25° and (c) 50°. (d) Normalized far-field radiation patterns.

phase compensation condition described in (1), a clear transformation from the cylindrical wave front to a plane wave front is observed. As shown in Fig. 2(d), the SLLs for 0° and 25° steering angles are -12.7 dB and -8.3 dB, respectively, showing a notable decrease compared to amplitude-binary FZP antennas reported in [23] and [24]. As shown in Fig. 2(c), the feeding antenna is rotated by 50° and moved down by 0.37 wavelength from its original position. Note that only the feeding antenna 1 is located at the center axis, the other two need an offset from the center axis. This 0.37-wavelength

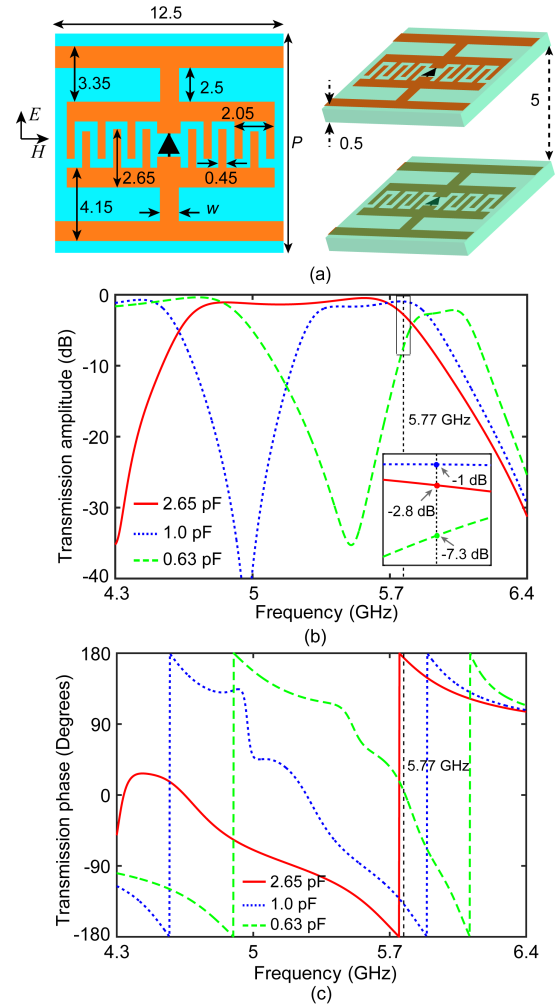


FIGURE 3. Metasurface unit cell and simulated transmission performance at normal incidence. (a) Geometrical structure of the unit cell. Unit in mm. (b) Transmission amplitude. (c) Transmission phase.

offset is determined by the width of the feeding antennas. In Fig. 2(d), it is seen that although the incident wave front shows a slight misalignment with the conformal lens, a beam steered to 50° with SLL better than -12 dB can still be observed. These results imply that if three (or more) antennas can be used to illuminate different regions of conformal lens, a wide-angle steering range with satisfactory SLLs can be obtained.

III. DESIGN

In this work, the conformal lens is designed with two layers of metasurfaces based on the unit cells previously used in [12] and [23], as shown in Fig. 3(a). Details of the modeling and the design procedure of unit cell can be found in [23]. The metallic unit cell is printed on a 0.5 mm-thick F4B substrate with a dielectric constant of 2.55 and a loss tangent of 0.003. The period of metasurface unit cell is around $\lambda/4$, in which λ is the wavelength at 5.75 GHz. Each unit cell is embedded with a microwave varactor, Skyworks SMV1405, to tune its transmission phase. The junction capacitance of

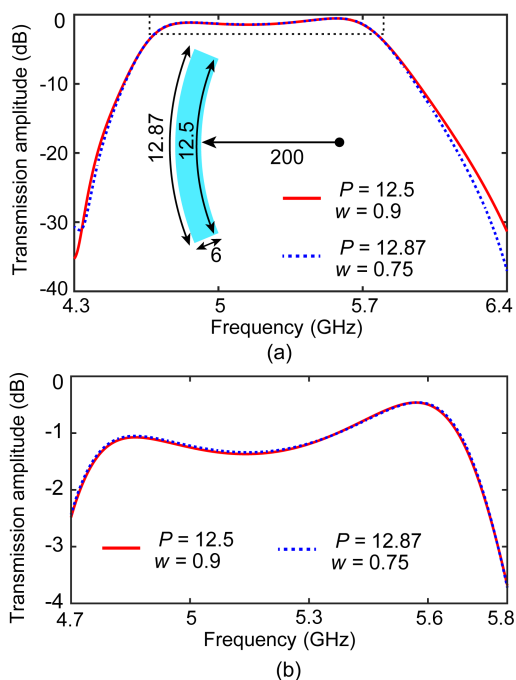


FIGURE 4. Transmission performance with different unit cell periods. (a) Transmission amplitude. (b) Zoom-in of the passband.

this diode decreases from 2.6 pF to 0.6 pF when DC bias voltage increases from 0 V to 30 V. Two layers of such metasurfaces separated by a 5-mm air gap was used to construct the conformal lens.

Full-wave simulations were performed with the CST Microwave Studio™ based on the SPICE model of the SMV1405 varactor. With the dimensions shown in Fig. 3(a), the simulated transmission amplitude and phase at the normal incidence are shown in Fig. 3(b) and 3(c), respectively. It is seen that, with 2.65-pF junction capacitance, two-layer metasurface exhibits two transmission maximum points in the band of 4.3–6.4 GHz, resulting in a much wider passband compared to that of the single-layer metasurface reported in [23]. This increases the possibility to obtain a wide range of phase tunability in the same passband. As seen in Figs. 3(b) and 3(c), with the decrease of the junction capacitance from 2.65 pF to 0.63 pF, the passband moves to higher frequencies. A phase shift around 192° can be obtained at 5.77 GHz with the maximum transmission loss of -7.3 dB. The insertion loss can be further reduced by using varactors with higher quality factor.

Note that the period of unit cells in the inner layer is slightly smaller (12.5 mm) than outer-layer ones (12.87 mm) due to the 5-mm radius difference. By slightly optimizing the geometric parameter w (0.9 mm and 0.75 mm for inner and outer layers, respectively), the transmission coefficient can remain unchanged in passband, as shown in Fig. 4.

IV. EXPERIMENT

A. FABRICATION

Using the optimized geometries, a two-layer cylindrical metasurface lens was fabricated, as shown in Fig. 5. Three

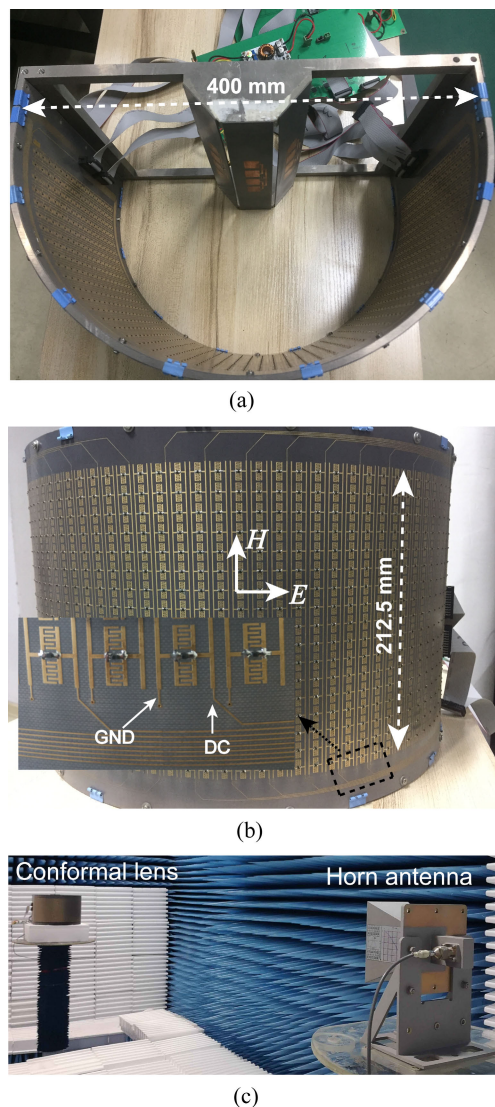


FIGURE 5. Fabricated metasurface cylindrical lens antenna and experimental setup. (a) Top view. (b) Front view. (c) Experimental setup.

identical feeding sources, each made of a 1×4 linear microstrip patch array, are used to illuminate the different regions of the conformal lens in the normal (source 1) and $\pm 50^\circ$ (sources 2 and 3) directions.

The fabricated conformal lens consists of two flexible metasurface layers, which were fixed on a 5-mm-thick aluminum supporter. Each metasurface layer consists of 850 unit cells, with 50 cells in a row and 17 cells in a column. Adjacent unit cells in the vertical direction are connected in parallel while isolated in the circumferential direction. In this way, each column can be individually controlled by a DC bias voltage. As shown in the inset of Fig. 5(b), the two vertical wires were connected to DC bias line and the ground line, respectively, so that all the diodes can be reversely biased. The bias lines were mounted along the upper and lower edges of the metasurface layers, and were connected to the control circuit by flexible cables, as shown in Figs. 5(a) and 5(b). In this work, the DC bias voltages were provided by a simple control

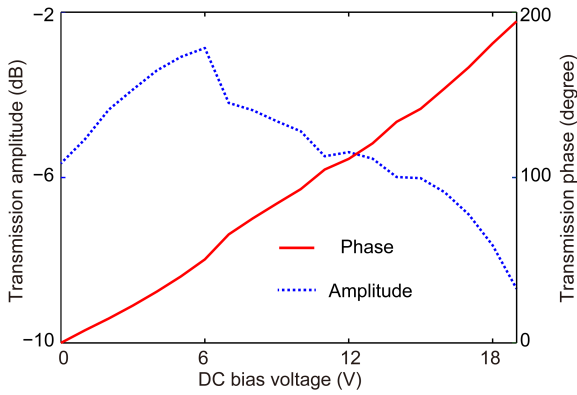


FIGURE 6. Measured transmission amplitude and phase of fabricated cylindrical lens at 5.75 GHz.

board based on a micro-controller unit (MCU) and eight 8-channel digital-to-analog converters (DACs), i.e., Texas Instruments DAC7718. Each DAC channel can individually output a DC voltage between 0 V to 30 V.

B. MEASUREMENT

The experimental measurements were performed in an anechoic chamber. The experimental setup is shown in Fig. 5(c). The conformal lens fed by three linear feeding sources was placed on a turntable, functioning as the transmitting antenna, and a reference horn antenna was placed in the far-field range, acting as the receiver. The measurement of transmission coefficient was performed in two steps. First, when the conformal lens was absent, the transmission between feeding antenna 1 and the horn antenna was measured, and the measured transmission amplitudes and phases were used as the calibration measurement. Then, the same measurements were repeated when the metasurface lens was installed and biased with same voltages. Note that in each step, only feeding antenna 1 was involved. The remaining antennas were connected with matched coaxial loads. The measured transmission amplitude and phase at 5.75 GHz are shown in Fig. 6. It is seen that a phase shift range of 195° can be obtained when DC bias voltage increases from 0 V to 19 V. In previous work [15], [18], [23], it has been shown that metasurface unit cells with 180° phase coverage is sufficient to implement dynamic beam steering. Compared to the simulated transmission loss, the increased loss may come from the reflection due to the bias lines and the metallic frame used to fix the metasurface, as shown in Figs. 5(a) and 5(b).

Based on the above phase tunability, a phase-correction conformal lens can be realized. Fig. 7(a) shows the S-parameters of lens antenna measured at 0° radiation angle. It is seen that around 5.75 GHz, the reflection coefficients are below -10 dB, and the isolation between adjacent feeding antennas is less than -20 dB. Note that the conformal metasurface is electrically large and comprised of thousands of unit cells with high-density interdigital structures. Full-wave simulation to this surface is impractical. Fig. 7(b) shows the beam collimation effect due to the DC-controlled conformal

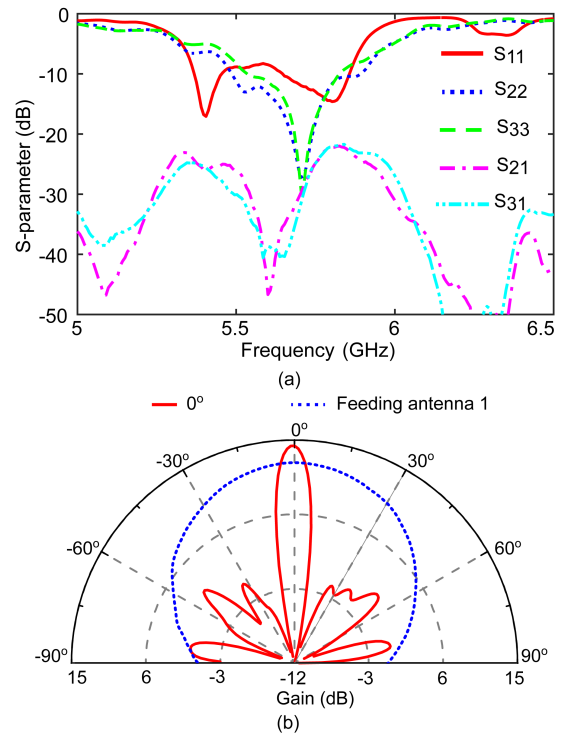


FIGURE 7. Measured S-parameters and radiation patterns at 0° radiation angle. (a) S-parameters. (b) radiation patterns at 5.75 GHz.

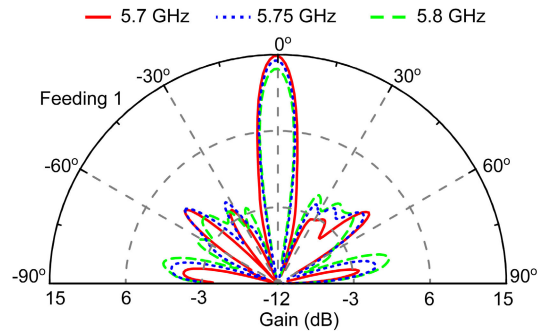


FIGURE 8. Measured radiation patterns at different operating frequencies.

lens. Compared with the 72° beamwidth of feeding antenna, the beamwidth of lens antenna is around 8°, significantly narrowed by the focusing effect of the conformal lens. Fig. 8 shows the radiation patterns of lens antenna at different operating frequencies. Within an instantaneous bandwidth of 100 MHz, similar beam collimation effect can be observed with the gain variation within 1.7 dB.

Fig. 9 shows the steered beams when the conformal lens was illuminated by the feeding antenna 1 at 5.75 GHz. The gain decreased from 14.3 dB to 12.2 dB when the main beam was steered from 0° to 30°. For the radiation patterns pointing to 0°, 10°, 20° and 30°, the measured SLLs were -12.3 dB, -9.5 dB, -7.9 dB and -5.0 dB, respectively. Due to the geometric symmetry, similar beam steering performance was observed in the negative direction, as shown in Fig. 9(b). Note

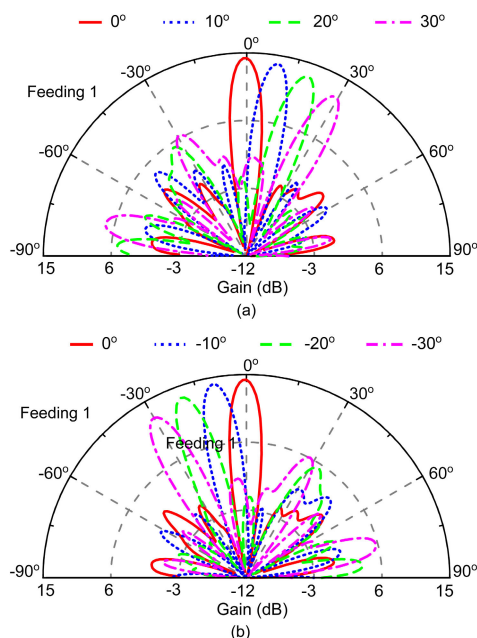


FIGURE 9. Beam steering performance at 5.75 GHz utilizing feeding antenna 1. (a) Positive direction. (b) Negative direction.

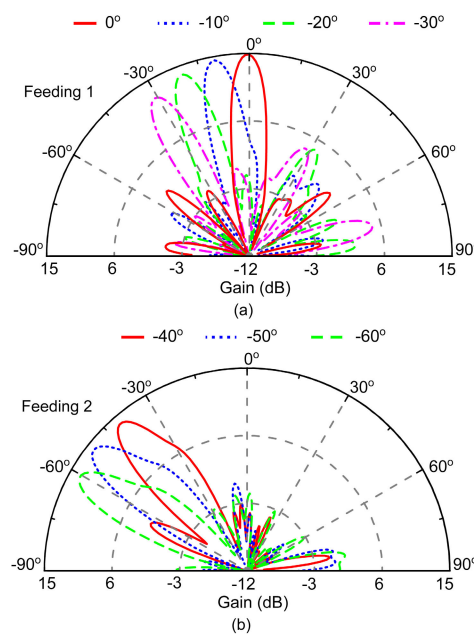


FIGURE 11. Beam steering performance at 5.7 GHz utilizing different feeding antennas. (a) Feeding antenna 1. (b) Feeding antenna 2.

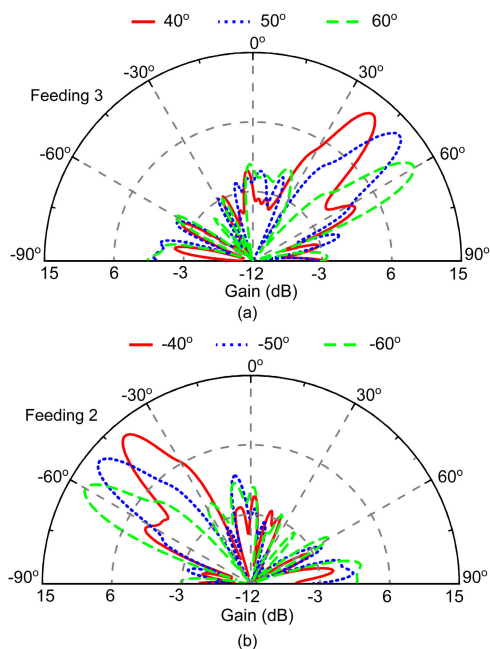


FIGURE 10. Beam steering performance at 5.75 GHz utilizing different feeding antennas. (a) Feeding antenna 3. (b) Feeding antenna 2.

that the above SLLs at $\pm 30^\circ$ are not satisfactory. This can be effectively improved by increasing the number of feeding antennas so that each antenna is responsible for a narrower steering region.

Fig. 10 (a) shows the beam steering performance due to the feeding antenna 3 at 5.75 GHz. At 50° deflection angle, the measured gain was 13 dB with a beamwidth of 10° . Compared to the 0° deflection angle, the beamwidth shows a slight increase due to the truncation effect of fabricated

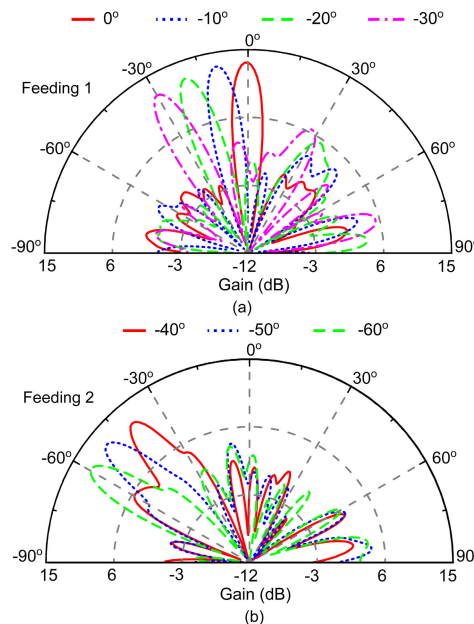


FIGURE 12. Beam steering performance at 5.8 GHz utilizing different feeding antennas. (a) Feeding antenna 1. (b) Feeding antenna 2.

lens. At 40° , 50° and 60° pointing angles, the measured SLLs were -9.6 dB, -12.2 dB, -10.5 dB, respectively. Similarly, with the feeding antenna 2, Fig. 10(b) shows the measured radiation patterns with main beams steered to the negative direction. These results demonstrate that the beam steering range can be readily expanded by simply increasing the number of feeding sources. Fig. 11 and Fig. 12 show the beam steering performance at 5.7 GHz and 5.8 GHz, respectively. Similar beam steering performance is observed within an instantaneous bandwidth of 100 MHz.

The above simulation and experimental results verified the effectiveness of proposed method. Taking advantage of 195° phase tunability provided by two-layer conformal metasurface lens, wide-angle beam steering was implemented with a simple structure. Compared with [23] and [24], both the beam steering range and the SLL are notably improved. Compared with conventional phased arrays relying on feeding networks and RF front ends integrated with phase shifters, amplifiers and attenuators [34], the proposed conformal lens is simple structured, cost effective and easy to control.

The measured maximum gain of the proposed conformal lens antenna is 14.3 dB, corresponding to an aperture efficiency of 6.8% for a uniform field illumination on the entire conformal lens (412 mm \times 215.5 mm). The relative low aperture efficiency is due to the large insertion loss and unfully illuminated aperture of metasurface lens. The 3-dB beamwidths of the feeding antenna in the horizontal and vertical planes are 72° and 23° , respectively. Therefore, the illuminating area can be estimated around 242 mm \times 84 mm, corresponding to a directivity of 19.7 dB. Considering the insertion loss of the metasurface lens between $-3\sim -8.5$ dB, the measured 14.3 dB gain is reasonable.

In order to improve the antenna efficiency in the future, varactors with lower loss can be used to build the conformal lens. Furthermore, the linear feeding source with higher gain can be used to illuminate the conformal lens.

V. CONCLUSION

A C-band conformal lens antenna capable of wide-angle beam steering was analyzed, simulated and experimentally demonstrated. Assisted with 195° phase tunability provided by the DC-controlled two-layer metasurfaces, such a wide-angle beam steering antenna can be implemented with a simple structure. Taking advantage of this conformal structure, the beam steering range can be conveniently expanded by increasing the number of feeding sources. Without complex feeding networks, this conformal lens can be easily and cost-effectively realized. The proposed approach can be extended to higher frequencies, enabling potential applications such as millimeter-wave wide-angle beam steering and multiple-input and multiple-output (MIMO) communication.

REFERENCES

- [1] R. J. Mailloux, *Phased Array Antenna Handbook*, 2nd ed. Norwood, MA, USA: Artech House, 2005.
- [2] C. A. Balanis, *Antenna Theory: Analysis and Design*, 2nd ed. New York, NY, USA: Wiley, 1997.
- [3] A. Navarro and K. Chang, *Integrated Active Antennas and Spatial Power Combining*. New York, NY, USA: Wiley, 1996.
- [4] F. Costa, A. Monorchio, S. Talarico, and F. M. Valeri, "An active high-impedance surface for low-profile tunable and steerable antennas," *IEEE Antennas Wireless Propag. Lett.*, vol. 7, pp. 676–680, 2008.
- [5] P. Deo, A. Mehta, D. Mirshekar-Syahkal, and H. Nakano, "An HIS-based spiral antenna for pattern reconfigurable applications," *IEEE Antennas Wireless Propag. Lett.*, vol. 8, pp. 196–199, 2009.
- [6] D. F. Sievenpiper, J. H. Schaffner, H. J. Song, R. Y. Loo, and G. Tagonan, "Two-dimensional beam steering using an electrically tunable impedance surface," *IEEE Trans. Antennas Propag.*, vol. 51, no. 10, pp. 2713–2722, Oct. 2003.
- [7] Y. Yashchyshyn and J. W. Modelski, "Rigorous analysis and investigations of the scan antennas on a ferroelectric substrate," *IEEE Trans. Microw. Theory Techn.*, vol. 53, no. 2, pp. 427–438, Feb. 2005.
- [8] T. F. Gallacher, R. Sondena, D. A. Robertson, and G. M. Smith, "Optical modulation of millimeter-wave beams using a semiconductor substrate," *IEEE Trans. Microw. Theory Techn.*, vol. 60, no. 7, pp. 2301–2309, Jul. 2012.
- [9] M. I. B. Shams, Z. Jiang, S. M. Rahman, L.-J. Cheng, J. L. Hesler, P. Fay, and L. Liu, "A 740-GHz dynamic two-dimensional beam-steering and forming antenna based on photo-induced reconfigurable Fresnel zone plates," *IEEE Trans. THz Sci. Technol.*, vol. 7, no. 3, pp. 310–319, May 2017.
- [10] S. Liu and T. J. Cui, "Concepts, working principles, and applications of coding and programmable metamaterials," *Adv. Opt. Mater.*, vol. 5, no. 22, Nov. 2017, Art. no. 1700624.
- [11] B. Ratni, A. de Lustrac, G.-P. Piau, and S. N. Burokur, "Reconfigurable meta-mirror for wavefronts control: Applications to microwave antennas," *Opt. Express*, vol. 26, no. 3, pp. 2613–2624, Feb. 2018.
- [12] T. Jiang, Z. Wang, D. Li, J. Pan, B. Zhang, J. Huangfu, Y. Salamin, C. Li, and L. Ran, "Low-DC voltage-controlled steering-antenna radome utilizing tunable active metamaterial," *IEEE Trans. Microw. Theory Techn.*, vol. 60, no. 1, pp. 170–178, Jan. 2012.
- [13] B. Orazbayev, M. Beruete, and I. Khromova, "Tunable beam steering enabled by graphene metamaterials," *Opt. Express*, vol. 24, no. 8, pp. 8848–8861, Apr. 2016.
- [14] Y. Zhang, Y. Feng, J. Zhao, T. Jiang, and B. Zhu, "Terahertz beam switching by electrical control of graphene-enabled tunable metasurface," *Sci. Rep.*, vol. 7, Oct. 2017, Art. no. 14147.
- [15] T. J. Cui, M. Q. Qi, X. Wan, J. Zhao, and Q. Cheng, "Coding metamaterials, digital metamaterials and programmable metamaterials," *Light, Sci. Appl.*, vol. 3, pp. 1–9, Oct. 2014.
- [16] M. R. M. Hashemi, S.-H. Yang, T. Y. Wang, N. Sepúlveda, and M. Jarrahi, "Electronically-controlled beam-steering through vanadium dioxide metasurfaces," *Sci. Rep.*, vol. 6, Oct. 2016, Art. no. 35439.
- [17] X. Wan, M. Q. Qi, T. Y. Chen, and T. J. Cui, "Field-programmable beam reconfiguring based on digitally-controlled coding metasurface," *Sci. Rep.*, vol. 6, Feb. 2016, Art. no. 20663.
- [18] L. Zhang, X. Q. Chen, S. Liu, Q. Zhang, J. Zhao, J. Y. Dai, G. D. Bai, X. Wan, Q. Cheng, G. Castaldi, V. Galdi, and T. J. Cui, "Space-time-coding digital metasurfaces," *Nature Commun.*, vol. 9, pp. 1–11, Oct. 2018.
- [19] X. Wan, T. Y. Chen, X. Q. Chen, L. Zhang, and T. J. Cui, "Beam forming of leaky waves at fixed frequency using binary programmable metasurface," *IEEE Trans. Antennas Propag.*, vol. 66, no. 9, pp. 4942–4947, Sep. 2018.
- [20] W. Pan, C. Huang, P. Chen, M. Pu, X. Ma, and X. Luo, "A beam steering horn antenna using active frequency selective surface," *IEEE Trans. Antennas Propag.*, vol. 61, no. 12, pp. 6218–6223, Dec. 2013.
- [21] M. Li and N. Behdad, "Fluidically tunable frequency selective/phase shifting surfaces for high-power microwave applications," *IEEE Trans. Antennas Propag.*, vol. 60, no. 6, pp. 2748–2759, Jun. 2012.
- [22] J. R. Reis, R. F. S. Caldeirinha, A. Hammoudeh, and N. Copner, "Electronically reconfigurable FSS-inspired transmitarray for 2-D beamsteering," *IEEE Trans. Antennas Propag.*, vol. 65, no. 9, pp. 4880–4885, Sep. 2017.
- [23] H. Li, D. Ye, F. Shen, B. Zhang, Y. Sun, W. Zhu, C. Li, and L. Ran, "Reconfigurable diffractive antenna based on switchable electrically induced transparency," *IEEE Trans. Microw. Theory Techn.*, vol. 63, no. 3, pp. 925–936, Mar. 2015.
- [24] H. Li, C. Ma, D. Ye, Y. Sun, W. Zhu, C. Li, and L. Ran, "Dual-band Fresnel zone plate antenna with independently steerable beams," *IEEE Trans. Antennas Propag.*, vol. 66, no. 4, pp. 2113–2118, Apr. 2018.
- [25] H. D. Hristov and M. H. A. J. Herben, "Millimeter-wave Fresnel-zone plate lens and antenna," *IEEE Trans. Microw. Theory Techn.*, vol. 43, no. 12, pp. 2779–2785, Dec. 1995.
- [26] J. Xu, Z. N. Chen, and X. Qing, "270-GHz LTCC-integrated high gain cavity-backed Fresnel zone plate lens antenna," *IEEE Trans. Antennas Propag.*, vol. 61, no. 4, pp. 1679–1687, Apr. 2013.
- [27] H. Li, G. M. Wang, H.-X. Xu, T. Cai, and J. Liang, "X-band phase-gradient metasurface for high-gain lens antenna application," *IEEE Trans. Antennas Propag.*, vol. 63, no. 11, pp. 5144–5149, Nov. 2015.
- [28] A. H. Abdelrahman, A. Z. Elsherbeni, and F. Yang, "Transmitarray antenna design using cross-slot elements with no dielectric substrate," *IEEE Antennas Wireless Propag. Lett.*, vol. 13, pp. 177–180, 2014.
- [29] M. A. Al-Joumayly and N. Behdad, "Wideband planar microwave lenses using sub-wavelength spatial phase shifters," *IEEE Trans. Antennas Propag.*, vol. 59, no. 12, pp. 4542–4552, Dec. 2011.

[30] M. N. Jazi, M. R. Chaharmir, J. Shaker, and A. R. Sebak, "Broadband transmitarray antenna design using polarization-insensitive frequency selective surfaces," *IEEE Trans. Antennas Propag.*, vol. 64, no. 1, pp. 99–108, Jan. 2016.

[31] N. Gagnon and A. Petosa, "Using rotatable planar phase shifting surfaces to steer a high-gain beam," *IEEE Trans. Antennas Propag.*, vol. 61, no. 6, pp. 3086–3092, Jun. 2013.

[32] S. M. A. M. H. Abadi and N. Behdad, "Design of wideband, FSS-based multibeam antennas using the effective medium approach," *IEEE Trans. Antennas Propag.*, vol. 62, no. 11, pp. 5557–5564, Nov. 2014.

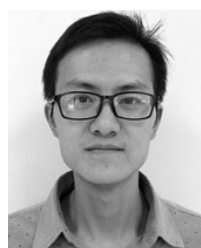
[33] M. Jiang, Z. N. Chen, Y. Zhang, W. Hong, and X. Xuan, "Metamaterial-based thin planar lens antenna for spatial beamforming and multi-beam massive MIMO," *IEEE Trans. Antennas Propag.*, vol. 65, no. 2, pp. 464–472, Feb. 2017.

[34] Y. Xia, B. Muneer, and Q. Zhu, "Design of a full solid angle scanning cylindrical-and-conical phased array antennas," *IEEE Trans. Antennas Propag.*, vol. 65, no. 9, pp. 4645–4655, Sep. 2017.

[35] L. Josefsson and P. Persson, *Conformal Array Antenna Theory and Design*. Piscataway, NJ, USA: IEEE Press, 2006.



DEXIN YE received the B.S. and Ph.D. degrees in electrical engineering from Zhejiang University, Hangzhou, China, in 2007 and 2013, respectively. As a Visiting Ph.D. Student, he visited The University of Arizona for six months and the Massachusetts Institute of Technology for one year during 2011 to 2013. From 2014 to 2016, he was a Postdoctoral Fellow and then became an Associate Professor, in 2016, with the Department of Information and Electronics Engineering, Zhejiang University. His recent research interests include artificial active metamaterials, perfectly matched layer, radio frequency, and microwave applications.



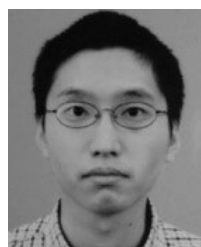
HUAN LI received the Ph.D. degree from Zhejiang University, Hangzhou, China, in 2016. He is currently working with Zhejiang University. His recent research interests include microwave circuits, antennas, measurement, and artificial metamaterials.



JIANGTAO HUANGFU received the B.S. and Ph.D. degrees in electrical engineering from Zhejiang University, Hangzhou, China, in 1999 and 2004, respectively. In July 2004, he became a Lecturer with the Department of Information and Electronic Engineering, Zhejiang University. Since 2006, he has served as an Associate Professor with Zhejiang University, where he is currently with the Laboratory of Applied Research on Electromagnetics (ARE). He was a Visiting Scientist with the Massachusetts Institute of Technology, Cambridge, MA, USA, in 2007. He was also a Visiting Scientist with the California Institute of Technology, Pasadena, CA, USA, in 2013 and 2014. His research interests focus on RF and microwave circuits, antennas, and microwave metamaterials.



CHAO MA received the B.S. degree from Zhejiang University, Hangzhou, China, in 2015, where he is currently pursuing the Ph.D. degree with the Laboratory of Applied Research on Electromagnetics (ARE). His research interests include antenna and microwave circuits.



FAZHONG SHEN received the B.S. and Ph.D. degrees from Zhejiang University, Hangzhou China, in 2008 and 2013, respectively. He is currently working with Zhejiang University. His research interests include measurement and imaging of material property and wireless power transfer.



CHANGZHI LI (S'06–M'09–SM'13) received the B.S. degree in electrical engineering from Zhejiang University, Hangzhou, China, in 2004, and the Ph.D. degree in electrical engineering from the University of Florida, Gainesville, FL, USA, in 2009.

From Summer 2007 to 2009, he was with Alereon Inc., Austin, TX, USA, and Coherent Logix Inc., Austin, where he was involved with ultrawideband (UWB) transceivers and software-defined radio. He joined Texas Tech University as an Assistant Professor, in 2009, and became an Associate Professor, in 2014. His research interests include biomedical applications of microwave/RF, wireless sensor, and analog circuits.

Dr. Li received the NSF Faculty Early CAREER Award, in 2013, the ASEE Frederick Emmons Terman Award, in 2014, the IEEE-HKN Outstanding Young Professional Award, in 2014, and the IEEE MTT-S Graduate Fellowship Award, in 2008. He also received nine best conference/student paper awards as the author/advisor in IEEE-sponsored conferences. He served as the TPC Co-Chair for the IEEE Wireless and Microwave Technology Conference (WAMICON), in 2012 and 2013. He was an Associate Editor for the IEEE TRANSACTIONS ON CIRCUITS AND SYSTEMS—II: EXPRESS BRIEFS, in 2014 and 2015. He is an Associate Editor of the IEEE TRANSACTIONS ON CIRCUITS AND SYSTEMS—I.



KUIWEN XU received the B.S. degree from Hangzhou Dianzi University, Hangzhou, China, in 2009, and the Ph.D. degree from Zhejiang University, China, in 2014. He visited the National University of Singapore, from 2012 to 2013. He is currently working with Hangzhou Dianzi University. His recent research interests include smart array antennas and inverse scattering problem.



LIXIN RAN received the B.S., M.S., and Ph.D. degrees from Zhejiang University, China, in 1991, 1994, and 1997, respectively. He became an Assistant Professor, in 1997, an Associate Professor, in 1999, and a Full Professor, in 2004, all with the Department of Information and Electronics Engineering, Zhejiang University. He is currently the Director of the Laboratory of Applied Research on Electromagnetics (ARE). In 2005, 2009, and 2012, he visited the Massachusetts Institute of Technology as a Visiting Scientist. He is a coauthor of over 140 peer-reviewed articles, and the Inventor of over 40 licensed patents. His research interests include wireless sensing and imaging, new concept antennas, advanced radio frequency, microwave and terahertz systems, and artificial microwave media.



TAYEB A. DENIDNI received the M.Sc. and Ph.D. degrees in electrical engineering from Laval University, Quebec City, QC, Canada, in 1990 and 1994, respectively. From 1994 to 2000, he was a Professor with the Engineering Department, Université du Québec in Rimouski (UQAR), Rimouski, QC, Canada, where he founded the Telecommunications Laboratory. Since 2000, he has been with the Institut National de la Recherche Scientifique (INRS), University of Quebec, Montreal, QC, Canada. He founded the RF Laboratory, INRS-Energie, Matériaux et Télécommunications (INRS-EMT), Montreal. He has extensive experience in antenna design. He served as a Principal Investigator on many research projects sponsored by NSERC, FCI, and numerous industries. His current research areas of interest include reconfigurable antennas using electromagnetic bandgap and frequency-selective surface structures, dielectric resonator antennas, meta-material antennas, adaptive arrays, switched multi-beam antenna arrays, ultra-wide band antennas, microwave, and development for wireless communications systems.

• • •